Adsorption Kinetics of Rigid 4-Mercaptobiphenyls on Gold

Sheng Liao, Yitzhak Shnidman, and Abraham Ulman*

Contribution from the Department of Chemical Engineering, Chemistry and Materials Science, Polytechnic University, and the NSF MRSEC for Polymers at Engineered Interfaces, Six Metrotech Center, Brooklyn, New York 11201

Received February 23, 1999. Revised Manuscript Received October 26, 1999

Abstract: We have presented the first experimental evidence that the molecular dipole and the electron density on the S-atom affect the adsorption process of thiols on gold. The adsorption kinetics of five rigid 4-mercaptobiphenyls onto a polycrystalline gold surface has been studied by the quartz crystal microbalance (QCM) technique. The kinetics data cannot be fitted to the Langmuir equation because it does not take interadsorbate interactions into consideration. A new lattice-gas adsorption model was developed that approximates the chemisorbed layer of interacting mercaptobiphenyls as lattice-gas particles with pair interactions between nearest-neighbor sites. The interacting lattice-gas model produces much better fits to experimental data and provides quantitative estimates of the strength of the chemisorption potential and the dipolar interactions, as well as of the rate constants. The formation of self-assembled monolayers (SAMs) from mercaptobiphenyls in toluene solutions is faster than that of *n*-alkanethiols, unless strong electron-attracting groups are substituted at the 4′-position. From the QCM measurements combined with ellipsometric data, we found that the initial adsorption rate constants at room temperature were directly related to the molecular dipole moment. The larger the dipole moment ($|\Delta\sigma|$) is, the more repulsive the intermolecular interactions (ϵ), and the slower the overall rate constant (Γ). The chemisorption potential (μ_s) is bigger than for alkanethiolate, probably because the S-gold bond is stronger. The plot of μ_s vs $|\Delta\sigma|$ shows a maximum, suggesting that μ_s includes the contributions of both the S-gold bond strength and the intermolecular repulsion.

Introduction

Over the past fifteen years, self-assembled monolayers (SAMs) have attracted much attention because of interest in two-dimensional molecular assemblies, and because of their potential applications in molecular devices, sensors, surface engineering, and more.[1] A variety of methods have been applied to the structural studies of these films,[2−10] providing some understanding of film structure at the molecular level. However, the intrinsic nature of the adsorption process still remains unclear. A better knowledge of the SAM-formation process may help improve the properties of these monolayer films, and allow molecular design of their composition.

Different groups have carried out the adsorption kinetics studies of thiols on gold.[11−16] Bain and co-workers used ellipsometry and contact angle measurements to follow the adsorption kinetics of octadecanethiol ($CH_3(CH_2)_{17}SH$) from ethanol solutions with different concentrations.[17] For 10 μM thiol concentration, film thickness increased up to 19 Å within the first 2 min, following by several hours of annealing process. Similarly, Ellis and co-workers, using reflection/absorption infrared spectroscopy (RAIRS), observed a two-step process.[18] They found that even with very dilute solutions of long-chain alkanethiols ($CH_3(CH_2)_{21}SH$), the main process of film formation is quite fast (∼1 min), and that the second step, which they called "ordered domain formation," is much slower. In these ex situ measurements, removing the substrate from the thiol solution may have interrupted the adsorption process, and therefore the results may not unveil the real nature of the SAM formation process. More recently, quartz crystal microbalance (QCM) has been used to study the formation process of SAMs in situ.[13,19,20] The QCM is very sensitive to mass-changes as

* To whom correspondence should be directed. Telephone: (718) 260-3119. Fax: (718) 260-3125. E-fax: (810) 277-6217. E-mail: aulman@duke.poly.edu.

(1) Ulman, A. *Chem. Rev.* **1996**, *96*, 1533−1554. (b) Ulman, A. *An Introduction to Ultrathin Organic Films;* Academic Press: Boston, 1991.
(2) Porter, M. D.; Bright, T. B.; Allara, D. L.; Chidsey, C. E. D. *J. Am. Chem. Soc.* **1987**, *109*, 3559.
(3) Widrig, C. A.; Alves, C. A.; Porter, M. D. *J. Am. Chem. Soc.* **1991**, *113*, 3, 2805.
(4) Alves, C. A.; Smith, E. L.; Porter, M. D. *J. Am. Chem. Soc.* **1992**, *114*, 1222.
(5) Nuzzo, R. G.; Zegarski, B. R.; Dubois, L. H. *J. Am. Chem. Soc.* **1987**, *109*, 733.
(6) Laibinis, P.; Whitesides, G. M.; Parikh, A. N.; Tao, Y. T.; Allara, D. L.; Nuzzo, R. G. *J. Am. Chem. Soc.* **1991**, *113*, 7152.
(7) Walczak, M. M.; chung, C.; Stole, S. M.; Widrig, C. A.; Porter, M. D. *J. Am. Chem. Soc.* **1991**, *113*, 2370.
(8) Bryant, M. A.; Pemberton, J. E. *J. Am. Chem. Soc.* **1991**, *113*, 3629, and 8284.
(9) Finklea, H. O.; Avery, S.; Lynch, M.; Furtsch, T. *Langmuir* **1987**, *3*, 409.
(10) Strong, L.; Whitesides, G. M. *Langmuir* **1988**, *4*, 546. (b) Dubois, L. H.; Zegarski, B. R.; Nuzzo, R. G. *J. Chem. Phys.* **1993**, *98*, 678. (c) Fenter, P.; Eisenberg, P.; Li, J.; Camillone, N., III; Bernasek, S.; Scoles, G.; Ramanarayanan, T. A.; Liang, K. S. *Langmuir* **1991**, *7*, 3013. (d) Samant, M. G.; Brown, C. A.; Gordon, J. G., II. *Langmuir* **1991**, *7*, 437. (e) Chidsey, C. E. D.; Liu, G.; Rowntree, P.; Scoles, G. *J. Chem. Phys.* **1989**, *91*, 4421.
(11) Hähner, G.; Wll, Ch.; Buck, M.; Grunze, M. *Langmuir* **1993**, *9*, 1955.
(12) Bucher, J. P.; Santesson, L.; Kern, K. *Langmuir* **1994**, *10*, 979.
(13) Pan, W.; Durning, C. J.; Turro, N. J. *Langmuir* **1996**, *12*, 4469.
(14) Peterlinz, K. A.; Georgiadis, R. *Langmuir* **1996**, *12*, 4731.
(15) Schneider, T. W.; Buttry, D. A. *J. Am. Chem. Soc.* **1993**, *115*, 12391.
(16) Buck, M.; Grunze, M.; Eiser, F.; Fiser, J.; Trger, F. *J. Vac. Sci. Technol., A* **1992**, *10*, 926.
(17) Bain, C. D.; Troughton, E. B.; Tao, Y. Y.; Evall, J.; Whitesides, G. M.; Nuzzo, R. G. *J. Am. Chem. Soc.* **1989**, *111*, 321.
(18) Bensebaa, F.; Voicu, R.; Huron, L.; Ellis, T. H. *Langmuir* **1997**, *13*, 5335.
(19) Karpovich, D. S.; Blanchard, G. J. *Langmuir* **1994**, *10*, 3315.

10.1021/ja9905804 CCC: $19.00
Published on Web 04/05/2000

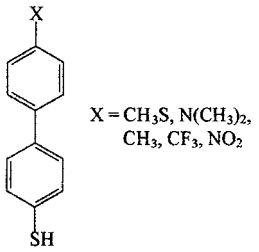

Figure 1. Mercaptobiphenyls.

small as several nanograms,[19] and thus may provide more accurate data on the *early* stage of the adsorption process. Shimazu and co-workers have used QCM for studies of structure-dependent ion-pairing and solvent uptake in self-assembled monolayers of 11-ferrocenyl-1-undecanethiol.[21] Karpovich and Blanchard have applied the QCM technique to observe the process of adsorption of long-chain *n*-alkanethiol*s* onto gold, and found that mass equilibrium for $CH_3(CH_2)_{17}SH$ and $CH_3(CH_2)_7SH$ SAMs, in micromolar solutions in hexane, was reached within the first minute.[19] Their estimated adsorption energy of aliphatic thiols onto gold (−5.5 kcal/mol) implies that the SAMs system is a highly dynamic one, that is, that molecules continuously adsorb and desorb. The scanning probe microscopy work carried out in McCarley group's supports this viewpoint.[22] They found that the macroscopic shape of SAMs on gold substrates exhibits changes over a few minutes time. However, it is still unclear what is the intermediate in the adsorption process, and what is the rate-determining step.

The shortcoming of the aliphatic systems is that, even for *n* -alkanethiolate SAMs, thermal disorder results in surface-*gauche* defects and thus in surface disorder. When surface dynamic processes exist, properties associated with surface chemical functionalities may be masked by conformational instabilities. Therefore, a preferred system for surface engineering will be one in which conformational disorder has been eliminated. This is achieved using rigid molecules, where surface functional groups have no conformational freedom and are "stuck" at the surface. 4-Mercaptobiphenyl derivatives (Figure 1) have the required rigidity to essentially eliminate end-group conformational dynamics processes.

Compared to aliphatic thiols, aromatic thiols are a less explored class of adsorbates, primarily due to the synthetic difficulties and poor solubility associated with multi-ring aromatic thiols. A number of complex aromatic structures have been prepared and assembled onto gold, including species such as isothiocyanoporphyrin,[23] (4-mercaptophenyl)-phthalimide,[24] and a porphyrin-linked fullerene derivative.[25] Rubinstein and co-workers assembled phenyl thiol, 4-biphenyl thiol, and 4-terphebyl thiol onto gold and reported that the latter two formed reproducible SAMs that were substantially more stable than those from phenyl thiol, presumably due to greater intermolecular packing interactions.[26] Molecular mechanics calculations predicted a herringbone structure for the adsorbed terphenyl thiol, where the molecules are oriented normal to the surface. Sita and co-workers have examined a related set of compounds where acetylenic units were located between the two phenyl rings.[27] Using scanning tunneling microscopy (STM), they observed the formation of ordered domains for the terphenyl species on gold. The data provided the first evidence for the formation of an ordered SAM that is not based on an *n*-alkanethiol derivative[27] and was consistent with the calculated structure for 4-terphenyl thiol on gold.[25] Tour and co-workers have synthesized an expanded collection of phenyl, biphenyl, and terphenyl derivatives, both with and without acetylenic units that link the phenyl rings, and characterized SAMs derived from them.[28] Tao and co-workers applied cyclic voltammetry (CV) to study the structure of aromatic-derivatized thiol monolayer on gold.[29] They showed that for phenyl-substituted thiols, the stability of a monolayer formed on gold depended on the location of the benzene ring in the alkyl chain, as well as on the length of this chain. Scoles and co-workers have studied the structure of a SAM of 4′-methyl-4-mercaptobiphenyl on gold, made from the gas phase, using helium and synchrotron X-ray diffraction techniques. They found that the molecules are tilted $<17°$ away from the surface normal, and that the SAMs are more thermally stable than their alkanethiolate counterpart ($C_8H_{17}SH$).[30]

We have been interested in SAMs of rigid thiols as building blocks for stable, molecularly engineered model surfaces. We have shown that mixed SAMs of 4′-hydroxy-4-mercaptobiphenyl and 4′-methyl-4-mercaptobiphenyl produced stable surfaces that retain their wetting properties after one-month storage under nitrogen.[31] Since biphenyls are planar in the solid state, in temperatures above 40 K,[32] and the benzene rings provide effective conjugation between different substituents at the 4′-positon and the thiol headgroups, these molecules may possess significant molecular dipoles that may affect the composition of mixed SAMs in equilibrium. Indeed, we have reported on the impact of solvent and dipole moment on the composition of mixed self-assembled monolayers of biphenyl thiols at equilibrium.[33,34] Because the biphenyl moiety allows conjugation between the substituent at the 4′-position and the thiophenol group, the electron-attracting/withdrawing properties of substituent should affect the acidity of this group. It should also affect the basicity of the thiophenolate conjugate base, and hence its hardness (or softness). Here we provide a detailed account of kinetics studies conducted using the quartz crystal microbalance (QCM). We will show that the adsorption kinetics of mercaptobiphenyls depends on the molecular dipole moment, while the desorption kinetics depends on the thiolate gold bond strength.

Experimental Section

Materials. Toluene was purchased from EM Science and used without further purification. All the rigid aromatic thiols were

(20) Yagi, I.; Sato, Y.; Uosaki, K *Langmuir* **1992**, *8*, 1385.
(21) Shimazu, K.; Yagi, I.; Uosaki, K. *J. Electroanal. Chem.* **1994**, *372*, 117.
(22) McCarley, R. L.; Dunaway, D. J.; Willicut, R. J. *Langmuir* **1993**, *9*, 2775.
(23) Han, W.; Li, S.; Lindsay, S. M.; Gust, D.; Moore, T. A.; Moore, A. L. *Langmuir* **1996**, *12*, 5742.
(24) Young, J. T.; Boerio, F. J.; Zhang, Z.; Beck, T. L. *Langmuir* **1996**, *12*, 1219.
(25) Akiyama, T.; Imahori, H.; Ajawakom, A.; Sakata, Y. *Chem. Lett.* **1996**, 907.
(26) Sabatani, E.; Cohen-Boulakia, J.; Bruening, M.; Rubinstein, I. *Langmuir* **1993**, *9*, 2974.
(27) Dhirani, A.-A.; Zehner, R. W.; Hsung, R. P.; Guyot-Sionnest, P.; Sita, L. R. *J. Am. Chem. Soc.* **1996**, *118*, 3319.
(28) Tour, J. M.; Jones, L., II; Pearson, D. L.; Lamba, J. J. S.; Burgin, T. P.; Whitesides, G. M.; Allara, D. L.; Parikh, A. N.; Atre, S. V. *J. Am. Chem. Soc.* **1995**, *117*, 9529.
(29) Tao, Y. T.; Wu, C. C.; Eu, J. Y.; Lin, W. L. *Langmuir* **1997**, *13*, 4018.
(30) Leung, T. Y. B.; Schwartz, P.; Scoles, G.; Schreiber, F.; Ulman, A. *Surf. Sci.*, submitted.
(31) Kang, J. F.; Jordan, R.; Ulman, A. *Langmuir* **1998**, *14*, 3983.
(32) von Laue, L.; Ermark, F.; Gölzhäuser, A.; Haeberlen, U.; Häcker, U. *J. Phys. Condens. Matter* **1996**, *8*, 3977.
(33) Kang, J. F.; Liao, S.; Jordan, R.; Ulman, A. *J. Am. Chem. Soc.* **1998**, *120*, 9662.
(34) Kang, J. F.; Liao, S.; Jordan, R.; Ulman, A. *Langmuir* **1999**, in press.

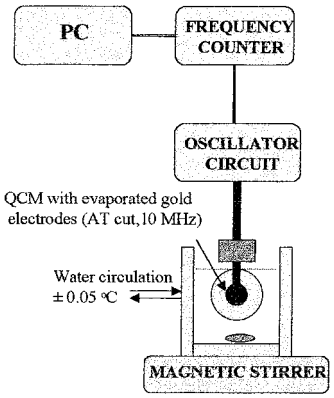

Figure 2. The QCM setup.

synthesized, purified by chromatography, crystallized, and analyzed in our laboratory. Details of synthesis and properties will be published elsewhere.[35]

Thickness Measurements. Thickness was estimated by ellipsometry using a Rudolph Research AutoELR ellipsometer, using an assumed refractive index of 1.462 for the SAM. The variation of measured thickness for biphenyl thiol monolayer was ~1−2 Å, with ±2 Å being the extreme case and ±1 Å the more observed one.

Kinetics Measurements. A QCM with a resonance frequency of ~10 MHz, sensitive to mass changes as small as several nanograms, was used. AT cut, polished quartz crystal plates with opposing surface electrodes were supplied by International Crystal Manufacturing (Oklahoma City, OK) with a nominal resonance frequency of 10 MHz. The vapor deposited electrodes were 100 Å of Cr beneath 1000 Å Au. The diameters of the crystal and electrodes were 0.318 in and 0.137 in, respectively. We purchased a lab oscillator specially designed by ICM. The QCM was connected to a HP 53131A universal counter that was interfaced with a PC computer (Figure 2).

The resonance frequency of the QCM is affected not only by mass uptaking but also by other factors such as the viscoelasticity of the forming monolayer, surface roughness, surface stress, temperature, and the dielectric constant of the solvent.[36] The microscopic roughness of the QCM electrode surface may trap liquid and result in an additional frequency shift. To avoid roughening the surface of polished crystal, we used a brief (1 min) exposure to an argon plasma to clean every new quartz crystal. The clean crystal was rinsed with toluene and immediately used. Every crystal was used only once. Reproducible results were obtained only with new crystal. The QCM crystal was suspended in a 250 mL-beaker circulated with water. A bath circulator (VWR Scientific Products) controlled the temperature with ±0.05 °C at the set temperature. A Teflon stirrer was used to ensure solution uniformity. The whole system was placed in a properly grounded Faraday cage to avoid any electrical noise. After every QCM experiment, the thickness of film was estimated by ellipsometry to make sure that it is monolayer. QCM responds to any uptaking of mass on the quartz crystal no matter if it is physically adsorbed or chemically adsorbed. Therefore, we used 190 mL of pure toluene to establish the baseline until the stability of ±1 Hz/hr was reached. To reduce any mechanical disturbance to the system, a small amount (1 mL) of concentrated thiol solution was introduced through a small Teflon tube, far away from the crystal. Before adding, the thiol solution was kept in the water bath to avoid any thermal disruption. The concentrations used here are from 7 to 500 μM. The temperature was set to 25.1 ± 0.05 °C.

Results and Discussion

QCM has been demonstrated by a few groups as a very useful technique in the study of adsorption kinetics from solution to a solid surface. The sensitivity to mass changes is determined by the crystal resonant frequency according to the Sauerbrey equation[37] that holds well in gas phase. The effect of exposing the QCM electrodes to liquids has been studied by Thompson and co-workers using network analysis and a series frequency measurements.[38,39] Karpovich and Blanchard in their paper discuss why the QCM can be used in the liquid phase.[19] Since frequency shifts result not only from the solute mass adsorbed on the quartz plates but also from the adsorption of solvent molecules, a baseline must be established, using the pure solvent. Thus, in the QCM experiment, after the addition of thiol to the solvent under equilibrium with the gold coated quartz crystal, toluene molecules must desorb to allow thiol molecules to adsorb, and the total frequency shift should be proportional to the available adsorption sites. Therefore, we do not attempt to extract absolute, but rather relative mass values. This treatment also reduces the effect of roughness differences among individual quartz crystal plates on the total frequency change.

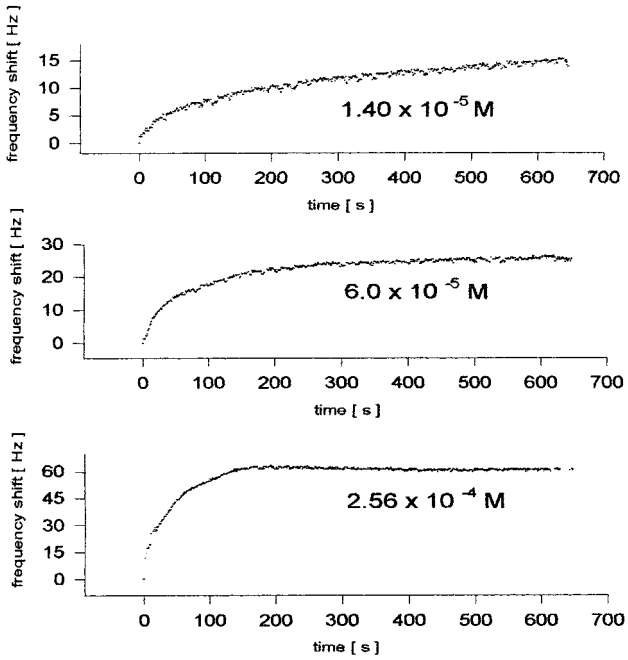

Figure 3. Concentration dependence of adsorption kinetics for CH_3S−Ph-Ph-SH.

We have examined biphenyl thiols (X-Ph-Ph-SH), with different substituents at the 4′-position (X = SCH_3, $N(CH_3)_2$, CH_3, CF_3, and NO_2). These substituents may be divided into an electron acceptor (NO_2, CF_3), and electron donor ($N(CH_3)_2$, SCH_3, CH_3) groups. The electron density on the adsorbing thiol S-atom should be smaller for the 4′-NO_2- than, for example, for the 4′-$N(CH_3)_2$-substituent. Four or five different concentrations were used for each thiol. For all concentrations, no multilayers could be detected by ellipsometry, and film thickness at the end of the experiment was between 14 ± 1 and 15 ± 1 Å. Figure 3 shows thiol concentration dependence of adsorption kinetics of CH_3S-Ph-Ph-SH, indicating that the mass equilibrium were reached after a period of few minutes, clearly *slower* than reported adsorption kinetics for *n*-alkanethiols.[19]

Before treating the data, we discuss the adsorption and desorption processes of thiols in the SAM formation process. So far, most researchers agree that the process of adsorption of thiols onto gold can be divided into two or three steps, the first is fast, and the following steps are much slower. Using the QCM, Karpovich and Blanchard found that mass equilibrium

(35) Kang, J. F.; Ulman, A., manuscript in preparation.
(36) Buttry, D. A.; Ward, M. D. *Chem. Rev.* **1992**, *92*, 1355.
(37) Sauerbrey, G. *Z. Phys* **1959**, *155*, 206.
(38) Yang, M.; Thompson, M. *Langmuir* **1993**, *9*, 802.
(39) Yang, M.; Thompson, M. *Langmuir* **1993**, *9*, 1990.

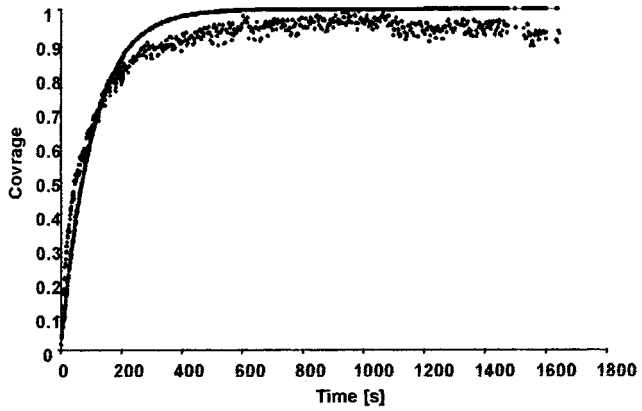

Figure 4. Langmuir fit for the adsorption kinetics of 4′-methylmercapto-4-mercapto-biphenyl on gold from 6.0×10^{-5} M solution in toluene.

for $CH_3(CH_2)_{17}SH$ and $CH_3(CH_2)_7SH$ in micromolar solutions of hexane was reached within the first minute (~9 s for 30 μM).[19] Buck and co-workers, using ethanol as the solvent, and employing a second-harmonic generation (SHG) technique to study in situ the kinetics of adsorption of $CH_3(CH_2)_{15}SH$, found that it took about 10 s to finish adsorption from a 45 μM solution.[40] On the basis of a combination of two techniques, SHG[37] and near-edge X-ray absorption fine structure (NEXAFS),[11] a two-step mechanism was suggested for the SAM formation from a 3 μM $CH_3(CH_2)_{21}SH$ solution. Thus, it took less than 10 s to finish the first step (sulfur adsorption) and 10 h to complete second step (orientation ordering). The orders of magnitude difference in time scale between these two steps justify that the first step can be treated separately. The kinetics of the first step is probably a mixture of physical and chemical adsorption processes—which cannot be separated—that is, governed by the surface−headgroup interaction, while that of the orientation-ordering step is governed by the interchain interactions. The following equation is used to describe the first step:

$$\text{X-Ph-Ph-SH}_{(sol)} \rightleftharpoons \text{X-Ph-Sh-SH} \cdot \text{Au}_n \rightleftharpoons \text{X-Ph-Ph-S}^-\text{Au}^+ \cdot \text{Au}_n + {}^1/_2\text{H}_2 \quad (1)$$

In this paper, we compare two different models to fit the QCM data. The first is the Langmuir isotherm model that assumes that there is no interaction between adsorbates. Karpovich and Blanchard[19] apply this model to fit the adsorption kinetics of alkanethiols on gold. It seems that their fit is successful. However, this may not be the case for 4-mercaptobiphenyl molecules. Figure 4 is the Langmuir fit for the adsorption kinetics of 4′-methylmercapto-4-mercaptobiphenyl on gold from 6.0×10^{-5} M solution toluene and Figure 5 is the Langmuir fit for the adsorption kinetics of 4′-trifluromethyl-4-mercaptobiphenyl on gold from 3.31×10^{-4} M solution in toluene. Notice that there are significant deviations from the Langmuir isotherm model especially for 4′-trifluro-4-mercapto-biphenyl. We defined *Err* as the deviation of fitted coverage from experimental data as

$$Err = \left[\frac{1}{n_t}\sum_{i=1}^{n_t}(\theta_f(t_i) - \theta_e(t_i))^2\right]^{1/2} \quad (2)$$

where $\theta_f(t_i)$ is the fitted coverage at time t_i, $\theta_e(t_i)$ is the experimental coverage ($\theta_e(t_i) = \Delta f(t_i)/\Delta f_{max}$ where $\Delta f(t_i)$ is the frequency shift at time t_i and Δf_{max} is the final maximum frequency shift), and n_t is the total number of data points. Table 1 summarizes the resulting Langmuir fits. It shows that the biggest deviation from the Langmuir isotherm model (largest *Err* value) occurs when the 4′-position of 4-mercaptobipyenyl is substituted with an NO_2 group. On the other hand, when 4′ position is CH_3S, there is the smallest deviation form the Langmuir isotherm model (*Err* has the smallest value). Figure 6 shows the observed adsorption kinetics, k_{obs}, as a function of concentration of 4′-methylmercapto-4-mercaptobiphenyl in toluene. Notice that even for the least polar molecule there is no linear relationship as is typical for the Langmuir adsorption mechanism. Considering that 4′-nitro-4-mercaptonbiphenyl has the largest dipole moment and 4′-methylmercapto-4-mercatonbiphenyl has the smallest dipole among these five molecules, Table 1 and Figure 6 suggest that the interaction between adsorbing molecules have to be taken into account, and the Langmuir isotherm does not fit well in this case.

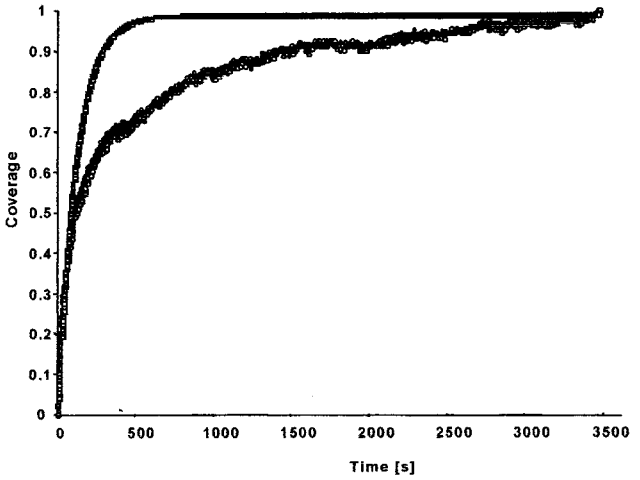

Figure 5. Langmuir fit for the adsorption kinetics of 4′-trifluoromethyl-4-mercaptobiphenyl on gold from 3.31×10^{-4} M solution in toluene.

Table 1. *Err* Values for Langmuir Fits of QCM Data for the Adsorption of Different 4-mercaptobiphenyls on Gold

4-Mercaptobiphenyl	k_a (mol sec^{-1})	k_d (mol sec^{-1})	*Err*
$NO_2-Ph-Ph-SH$	27	6.3×10^{-5}	0.106
$CF_3-Ph-Ph-SH$	148	1.1×10^{-4}	0.103
$N(CH_3)_2-Ph-Ph-SH$	191	1.7×10^{-4}	0.087
$CH_3-Ph-Ph-SH$	212	1.6×10^{-4}	0.093
$CH_3S-Ph-Ph-SH$	736	9.6×10^{-4}	0.073

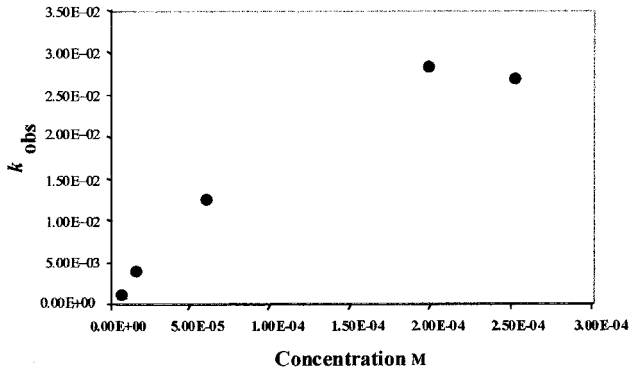

Figure 6. A plot of k_{obs} vs concentration of 4′-methyl-mercapto-4-mercaptobiphenyl in toluene.

(40) Buck, M.; Grunze, M.; Eiser, F.; Fiser, J.; Trger, F. *J. Vac. Sci. Technol., A* **1992**, *10*, 926−929.

Therefore, we have developed a new chemisorption model that takes interadsorbate interactions into consideration explicitly. We model the process of chemisorption of 4-mercaptobiphenyls from solution to the (111) gold surface as follows. We assume that:

(a) The energy of a single, isolated adsorbed molecule is lowered by μ_s (where $\mu_s > 0$) relative to the energy of the molecule in the bulk solution.

(b) Adsorbed molecules occupy the sites of a triangular lattice on the (111) surface of gold, and molecules occupying nearest-neighbor sites on that lattice have a pair interaction energy of $-\epsilon$.

(c) There is an energy barrier of ω for adsorption and $\omega + \mu_s$ for desorption of single, isolated molecules to/from the surface

Under these assumptions, the energy of the 4-mercaptobiphenyl molecules adsorbed to the (111) gold is approximated by the following lattice-gas Hamiltonian defined on the triangular lattice:

$$H = -\frac{1}{2}\epsilon\sum_{\vec{r}}\sum_{i=1}^{z} t_{\vec{r}}t_{\vec{r}+\hat{e}_i} - \mu_s\sum_{\vec{r}} t_{\vec{r}} \qquad (3)$$

where $t_{\vec{r}} = 1,0$ denotes that the site $\vec{r}$ is occupied or empty, respectively. Here $z = 6$ is the number of nearest-neighbors at each site (coordination number) for the triangular surface lattice of adsorption sites. Using $t_{\vec{r}} = (1 + s_{\vec{r}})/2$, where $s_{\vec{r}} = \pm 1$ are Ising pseudo-spins denoting occupied (empty) sites, the lattice-gas Hamiltonian above is equivalent (up to an energy constant) to an Ising Hamiltonian

$$H = -\frac{1}{8}\epsilon\sum_{\vec{r}}\sum_{i=1}^{z} s_{\vec{r}}s_{\vec{r}+\hat{e}_i} - \left(\frac{1}{2}\mu_s + \frac{1}{4}z\epsilon\right)\sum_{\vec{r}} t_{\vec{r}} \qquad (4)$$

We represent adsorption from solution as a Glauber (spin-flip) stochastic dynamic process. The transition rate for this process is assumed to be of the simple form $\varphi(\lambda) = \exp(-\lambda/2)$, where $\lambda = \Delta H_{\pm}/k_BT$ is the change in energy associated with the adsorption or desorption of a molecule at a single site, scaled by k_BT, the thermal energy. This satisfies the local detailed balance condition $\varphi(\lambda) = e^{-\lambda}\varphi(-\lambda)$, thus ensuring convergence to equilibrium at long times. Assuming translational invariance for the mean site occupancy, $\langle t_{\vec{r}}\rangle = n_{\vec{r}} \equiv n$, the time evolution of n is obtained from the master equation within a dynamic mean field approximation, as follows:

$$\frac{1}{\Gamma}\frac{dt}{dn} = (1-n)n_b \exp[(z\tilde{\epsilon}n + \tilde{\mu}_s)/2] - n(1-n_b)\exp[-(z\tilde{\epsilon}n + \tilde{\mu}_s)/2] \qquad (5)$$

where $\tilde{\mu}_s = \mu_s/k_BT$, $\tilde{\epsilon} = \epsilon/k_BT$, and n_b is the bulk solution occupancy, related to the bulk concentration by $n_b = \nu_m c_b$, where ν_m is a molecular volume. Here, $\Gamma \propto \exp(\omega/2k_BT)$ has the dimensions of inverse time $\Gamma = 1/\tau$, where τ is a microscopic relaxation time. At specified temperature T and bulk concentration c_b, the mean surface site occupancy (coverage) can be calculated by a numerical integration of eq 5, if the three parameters μ_s, ϵ, and Γ are known. Note that: (*a*) If $\epsilon = 0$, we recover the Langmuir adsorption equation. (*b*) At equilibrium, $dn/dt = 0$. Assuming $n_b \ll 1$, this leads to the following equation determining equilibrium surface occupancy n_{eq}

$$(1-n_{eq})n_b \exp\lfloor(z\tilde{\epsilon}n_{eq} + \tilde{\mu}_s)/2\rfloor - n_{eq}(1-n_b)\exp\lfloor-(z\tilde{\epsilon}n_{eq} + \tilde{\mu}_s)/2\rfloor = 0 \qquad (6)$$

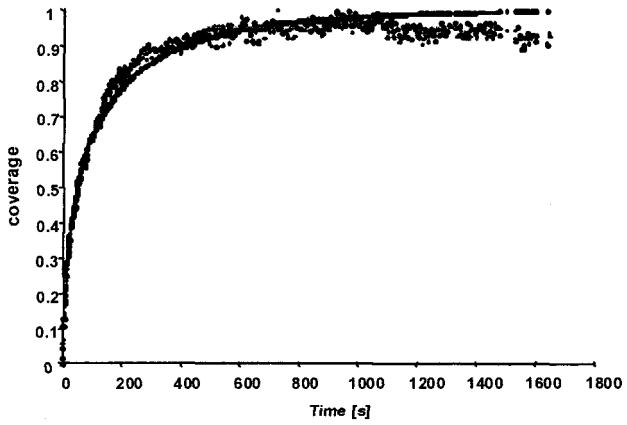

Figure 7. The chemisorption model fit for the adsorption kinetics of 4′-methylmercapto-4-mercaptobiphenyl from a 6.0×10^{-5} M solution in toluene.

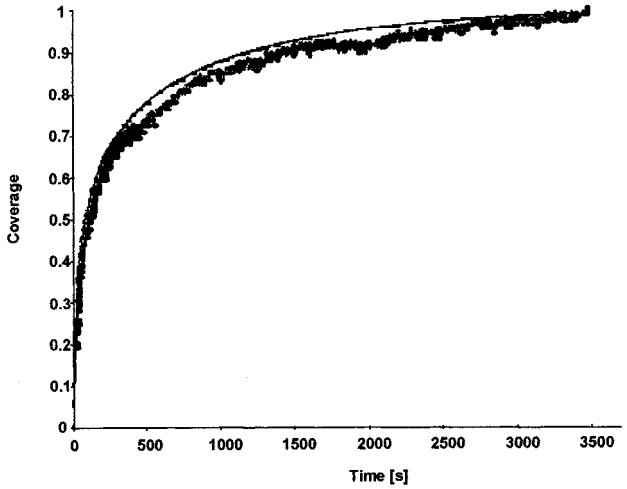

Figure 8. The chemisorption model fit for the adsorption kinetics of 4′-methylmercapto-4-mercaptobiphenyl from a 3.31×10^{-4} M solution in toluene.

or

$$(1-n_{eq})n_b - n_{eq}(1-n_b)\exp\lfloor-(z\tilde{\epsilon}n_{eq} + \tilde{\mu}_s)\rfloor = 0 \qquad (7)$$

We have performed least-squares fits of the three parameters μ_s, ϵ and Γ in eq 5 to relative coverage data obtained from QCM measurements. This was done by minimizing a cumulative square-error objective function (eq 2) obtained from the differences between mean site occupancies numerically integrated from eq 5 and the experimental QCM relative coverage time sequences. Each fit used data from a series of 2−4 experiments performed at the same temperature, and using the same adsorbates and solvents but 2−4 different bulk concentrations of the adsorbents.

Figures 7 and 8 are the chemisorption model fit for the adsorption kinetics of 4′-methylmercapto-4-mercaptobiphenyl and 4′-trifluromethyl-4-mercapto-biphenyl on gold from 6.0×10^{-5} M and 3.31×10^{-4} M solutions in toluene, receptively. We can see the fits are much improved. Table 2 shows that *Err* values are significantly smaller than those in Table 1.

It is important to point out that from the fit of the chemisorption model, the interaction parameter ϵ values for all the five biphenyls are negative which means the interactions between molecules are repulsive. If we use

$$|\Delta\sigma| = \Delta\sigma = \sigma_p{}^0(x) - \sigma_p{}^0(SCH_3) \qquad (8)$$

Table 2. Fitting of QCM Data for the Adsorption of Different 4-mercaptobiphenyls on Gold to the New Adsorption Model

4-Mercaptobiphenyl	σ_p^0	$\lvert\Delta\sigma\rvert$	*Err*	Γ (s^{-1})	ϵ (kcal/mol)	μ_s (kcal/mol)
NO_2−Ph−Ph−SH	0.81	0.87	0.064	0.0071	−2.44	10.10
CF_3−Ph−Ph−SH	0.53	0.59	0.025	0.0145	−2.29	12.20
$N(CH_3)_2$−Ph−Ph−SH	−0.32	0.26	0.048	0.0217	−1.95	12.39
CH_3−Ph−Ph−SH	−0.14	0.08	0.065	0.0310	−1.21	11.98
CH_3S−Ph−Ph−SH	−0.06	0	0.031	0.155	−1.08	11.41

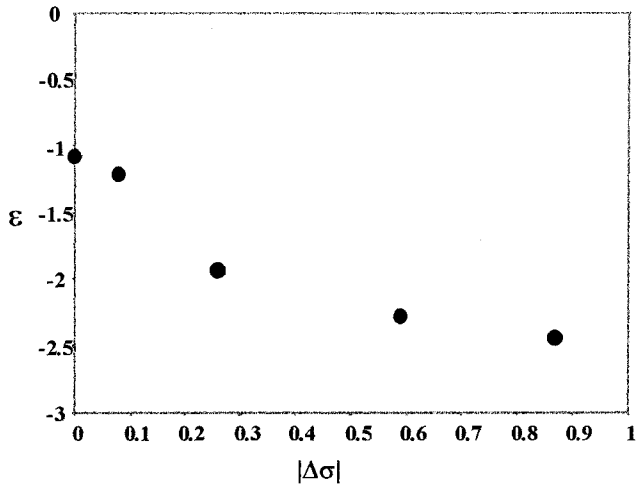

Figure 9. A plot of the interaction parameter ϵ against $|\Delta\sigma|$.

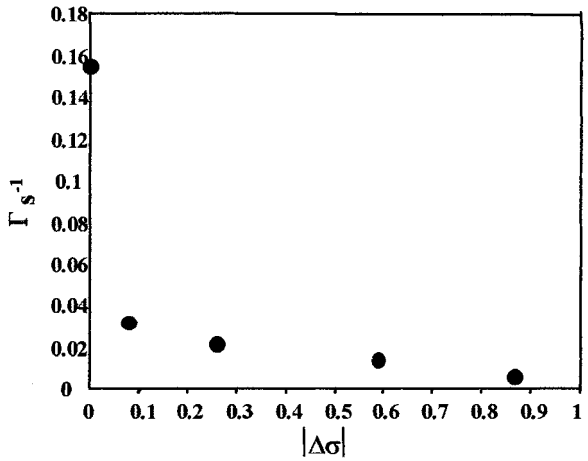

Figure 10. A plot of the overall rate constants Γ vs $|\Delta\sigma|$.

as the measure for the molecular dipole moment,[41] the plot of the interaction parameter ϵ against $|\Delta\sigma|$ Figure 9) shows that the molecule which has the bigger dipole moment has stronger repulsive force, which dominates over attractive van der Waals forces.

A plot of the rate constants Γ vs $|\Delta\sigma|$ (Figure 10) provides more information about the adsorption kinetics. It shows that the bigger the molecular dipole moment the slower are both the adsorption and desorption processes due to a barrier resulting from repulsive interaction. This means that the molecules with smaller dipole moment reach equilibrium faster.

Table 2 shows that adsorption of CH_3S-Ph-Ph-SH on gold is the fastest, while that of NO_2-Ph-Ph-SH the slowest (0.155, vs 0.0071). This suggests that increasing the electron-donating property of the substituent at the 4′-position accelerates the adsorption process. This acceleration can be due to both physisorption and chemisorption processes. In the physisorption process, the interaction between the approaching thiol and the gold surface may be manifested by the overlap of the sulfur nonbonded electrons with the gold empty orbitals. Thus, as the substituent at the 4′-position becomes a better electron donor, the electron density at the SH group increases and with that the strength of its interaction with the gold surface. We note that there is a correlation between the effect of the substituent on the electron density at the adsorbing sulfur and the molecular dipole moment. However, it is not possible to quantify their correlation given the kinetics data presented here.

As for the chemisorption, Sellers has suggested that the S−H bond breaks when the thiol is adsorbed at the on-top position of an Au(111) surface.[42] This is an oxidative addition reaction, in which the SH bond breaks homolytically, and where the intermediate, a gold(II) hydride [$RS^-Au^{2+}H^-$], immediately undergoes reductive elimination to the gold(I) thiolate [RS^--Au^+]:

$$R{-}S{-}H + Au_n \rightarrow [RS^-Au^{2+}H^-]{\cdot}Au_n \rightarrow [RS^-Au^+] + {}^1/_2H_2{\cdot}Au_n \quad (9)$$

While there has been no clear experimental evidence for the fate of the SH proton, we have never detected its presence in IR spectra of 4-mercaptobiphenyl SAMs, and XPS data (not shown here) exhibits one sulfur peak, suggesting a sulfur−gold bonding. If this mechanism is correct, the homolytic cleavage of the S−H bond will be slower when this bond is more polar (the proton more acidic). This is in complete agreement with the Γ values, and is the first experimental evidence that the electron density of the adsorbing sulfur affects adsorption kinetics. Why is the Γ value for CH_3 smaller than the corresponding value for $N(CH_3)_2$? The reason is probably because in the latter intermolecular dipolar interactions (ϵ) are stronger due to larger $|\Delta\sigma|$.

The chemisorption potential μ_s values from Table 2 are bigger than the ∼5.5 kcal/mol reported for alkanethiols.[19] This suggests that the chemical bond between the thiolate and gold is stronger for 4-mercaptonbiphenyl than that for alkanethiol. That can be understood based on the hard and soft acids and bases concept.[43−45] This concept proposes that reactions will occur most readily between species that are matched in hardness and softness. Hard bases prefer hard acids, and soft bases prefer soft acids. As electron density is withdrawn from the adsorbing sulfur atom, it becomes a softer base, which matches the soft Au^{1+} acid. Thus, if the structure is of biphenylthiolate (RS^-) on Au^{1+}−disulfides[46] cannot be formed if the biphenyl moieties are perpendicular to the surface, which is apparent from all FTIR studies[31], then the softer the thiolate the stronger its bond to the gold surface.

The plot of μ_s vs $|\Delta\sigma|$ (Figure 11) shows a maximum, suggesting that μ_s, which represents the excess energy of the adsorbate in the adsorbed state, includes both the sulfur−gold bond energy and the interadsorbate repulsion. These two are antagonistic, and since both increase with the decreasing electron density at the thiolate sulfur, the value of μ_s goes through a maximum. While μ_s represents a one-body interaction parameter in our model, higher-order interadsorbate interactions in the real system may be folded into such an effective parameter.

(41) For values of σ_p^0, see: March, J. *Advanced Organic Chemistry-Reactions, Mechanism, and Structure*, 2nd ed.; McGraw-Hill: New York, 1977.

(42) Sellers, H. *Surf. Sci.* **1993**, *294*, 99.
(43) Pearson, R. G.; Songstand, J. *J. Am. Chem. Soc.* **1967**, *89*, 1827.
(44) Pearson, R. G. *J. Chem. Edu.* **1968**, *45*, 581, 643.
(45) Ho, T. L. *Chem. Rev.* **1975**, *75*, 1.
(46) Fenter P.; Eberhardt, A.; Eisenberger, P. *Science* **1994**, *266*, 1216.

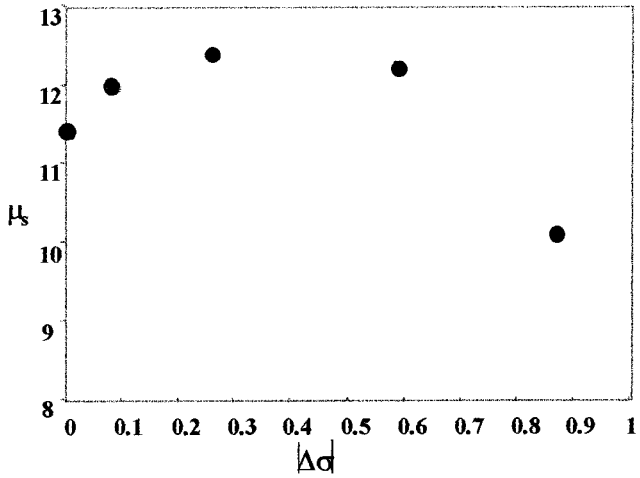

Figure 11. A plot of μ_s vs $|\Delta\sigma|$.

Conclusions

We have presented the first experimental evidence that the molecular dipole and the electron density on the S-atom affect the adsorption process of thiols on gold. The adsorption kinetics of five rigid 4-mercaptobiphenyls onto a polycrystalline gold surface has been studied by the quartz crystal microbalance (QCM) technique. The kinetics data cannot be fitted to the Langmuir equation because it does not take interadsorbate interactions into consideration. A new lattice-gas adsorption model was developed that approximates the chemisorbed layer of interacting mercaptobiphenyls as lattice-gas particles with pair interactions between nearest-neighbor sites. The interacting lattice-gas model produces much better fits to experimental data and provides quantitative estimates of the strength of the chemisorption potential and of the dipolar interactions, as well as of the rate constants. The formation of self-assembled monolayers (SAMs) from mercaptobiphenyls in toluene solutions is faster than that of *n*-alkanethiols, unless strong electron-attracting groups are substituted at the 4′-position. From the QCM measurements combined with ellipsometric data, we found that the initial adsorption rate constants at room temperature were directly related to the molecular dipole moment. The larger the dipole moment ($|\Delta\sigma|$) is, the more repulsive the intermolecular interactions (ϵ) and the slower the rate constant (Γ). The adsorption chemical potential (μ_s) is bigger than for alkanethiolate, probably because the S-gold bond is stronger. The plot of μ_s vs $|\Delta\sigma|$ shows a maximum, suggesting that μ_s includes the contributions of both the S-gold bond strength and the intermolecular repulsion.

Acknowledgment. This work was supported by the National Science Foundation through the MRSEC for Polymers at Engineered Interfaces.

JA9905804